

Article

# Organic Salts and Merrifield Resin Supported $[\text{PM}_{12}\text{O}_{40}]^{3-}$ (M = Mo or W) as Catalysts for Adipic Acid Synthesis

Jana Pisk<sup>1,2,\*</sup> , Dominique Agustin<sup>1,2,\*</sup>  and Rinaldo Poli<sup>1,3</sup> 

<sup>1</sup> Centre National de la Recherche Scientifique (CNRS), Laboratoire de Chimie de Coordination (LCC), Université de Toulouse, UPS, INPT, 205, route de Narbonne, 31077 Toulouse, France; rinaldo.poli@lcc-toulouse.fr

<sup>2</sup> Université de Toulouse, IUT P. Sabatier, Département de Chimie, Av. G. Pompidou, BP 20258, 81104 Castres CEDEX, France

<sup>3</sup> Institut Universitaire de France, 103, bd Saint-Michel, 75005 Paris, France

\* Correspondence: jana.pisk@chem.pmf.hr (J.P.); dominique.agustin@iut-tlse3.fr (D.A.); Tel.: +33-5-63-62-11-72 (D.A.)

Received: 1 February 2019; Accepted: 15 February 2019; Published: 21 February 2019

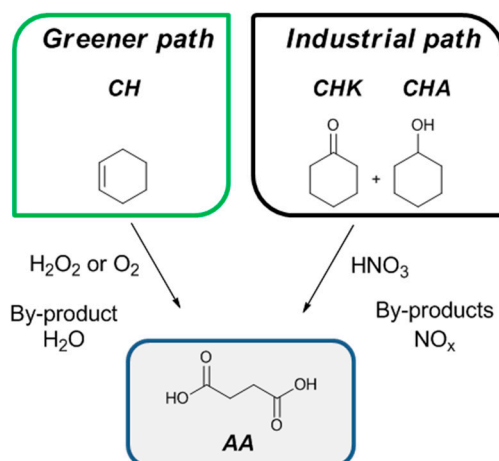


**Abstract:** Adipic acid (AA) was obtained by catalyzed oxidation of cyclohexene, epoxycyclohexane, or cyclohexanediol under organic solvent-free conditions using aqueous hydrogen peroxide (30%) as an oxidizing agent and molybdenum- or tungsten-based Keggin polyoxometalates (POMs) surrounded by organic cations or ionically supported on functionalized Merrifield resins. Operating under these environmentally friendly, greener conditions and with low catalyst loading (0.025% for the molecular salts and 0.001–0.007% for the supported POMs), AA could be produced in interesting yields.

**Keywords:** polyoxometalates; Merrifield resin; cyclohexene; adipic acid; organic solvent-free process

## 1. Introduction

Adipic acid (AA) is one of the reagents used for the production of nylon-6,6, a polymer that exhibits high mechanical strength, rigidity, and good thermal and chemical stability [1]. Most industrial processes for the AA production (2.3 Mtons/year) involve nitric acid oxidation of cyclohexanol (CHA) and/or cyclohexanone (CHK) [2,3]. This inexpensive acid, used in several industrial processes [4], however, leads to pollution, producing unwanted waste and various nitrogen oxides ( $\text{NO}_x$ ), including ca. 400 ktons of the greenhouse gas  $\text{N}_2\text{O}$  per year [5,6]. Although this emission can be significantly reduced using a thermal decomposition process [7,8], current academic and industrial process developments focus on cleaner technologies [2,3,9–11]. One possible alternative route for AA production is the selective oxidation of cyclohexene (CH) with hydrogen peroxide ( $\text{H}_2\text{O}_2$ ) [12,13] or molecular oxygen ( $\text{O}_2$ ) [14] as preferred oxidants (Scheme 1). Even though recent reports describe a very fast AA production under high pressure and high temperatures conditions [15–19], using membrane reactors [20] or microwave conditions [21], our research goal is to apply user-friendly and safe protocols (lower temperatures avoiding the  $\text{H}_2\text{O}_2$  decomposition, atmospheric pressure, one step reaction, recoverable catalyst), and to compare them with the classical protocols used in industrial processes.



**Scheme 1.** Proposed routes for the synthesis of adipic acid (AA).

Heteropolyoxometalates—inorganic compounds with general chemical formula  $[X_nM_pO_q]^{z-}$ , M being commonly Mo or W, and X being usually a main group element (Si, P, B)—were described as suitable for catalyst design at the atomic and molecular levels [22]. Among all structures, the one corresponding to the discrete assembly of 12 M around one X, with a general formula  $[XMo_{12}O_{40}]^{n-}$  (called Keggin), is very stable. Different isomers of Keggin polyoxometalates (POMs) can exist, according to the arrangement of the metal oxides around the heteroatom. Keggin-type POMs are efficient catalysts for liquid phase oxidation [23], due to their stability towards oxygen donors and their ability to incorporate different transition metals [24]. Immobilization of POMs through electrostatic interactions in insoluble polymer resins can lead to easier separation and recovery of the molecular catalysts [25,26]. Other interesting supports are  $SiO_2$  [27], mesoporous silica (SBA) [28,29] or certain macroporous resins [30]. Among the resins, the low-cost and relatively robust Merrifield resins (MR), originally developed for the solid-state synthesis of peptides [31], have the ability to undergo facile functionalization [25]. Even though many transition metal catalysts have been supported on MR for catalytic purposes [25,32,33], there is no report, to the best of our knowledge, on the application of such ionically supported POM-based catalysts for AA production.

The AA production from a mixture of CHA and CHK (so-called KA “ketone-alcohol” oil [34]) has previously been described using various homogeneous catalysts such as  $H_2WO_4$  [35] or Keggin-based POMs, i.e.,  $M_xPMo_{12}O_{40}$  (M = Ni, Co) [36],  $H_{3-2x}Co_xPMo_{12}O_{40}$  [37], or  $Y_{3-2x}Ni_xPMo_{12}O_{40}$  (Y = H or  $NH_4$ ,  $x = 0.25-1.5$ ) [38]. With  $(C_4H_9N)_3[PMo_{12}O_{40}]$ , AA (18% yield) and CHK were produced from CHA, while  $(C_4H_9N)_3[PW_{12}O_{40}]$  produced CHK only [39]. The replacement of the substrates (CHA, CHK) used in industrial processes by other starting substrates (CH, cyclohexane oxide CHO, 1,2-cyclohexanediol CHD), is guided by several economical parameters (substrate price, target yield, availability, time cost analysis, etc.). An attractive starting material, CH, was successfully converted to AA by aqueous  $H_2O_2$  using  $Na_2WO_4$  as a catalyst and the  $[CH_3(n-C_8H_{17})_3N]HSO_4$  phase transfer agent [40]. The oxidation of *trans*-CHD is another suitable pathway for AA production [3,10,41,42] providing the highest AA yields but CHD is the most expensive reagent among the listed substrates. On the other hand, CH is largely available by benzene hydrogenation [43–45] or by cyclohexane dehydrogenation [46–48] and, therefore, less expensive and more promising. Since CHD can be obtained by the oxidation of CH, a more direct and selective AA “one-pot” production from CH is of great interest.

Different heterogeneous catalysts based on calcined POMs [49], mesoporous solids [50], Ti-MMM-2 [51], Ce-SBA-15 [51], TAPO-5 [52], and Ti-AISBA-15 [53,54] were also tested for direct CH oxidation, the AA yield being improved by the stepwise addition of  $H_2O_2$  to the reaction mixture. The catalytic mechanism for the CH oxidation into AA through CHD was clarified with TAPO-5 as a catalyst [52], showing that *trans*-CHD was formed from cyclohexene oxide (CHO) while the *cis*-CHD

formation followed a radical mechanism. The CH oxidation to AA was also tested in CH<sub>3</sub>CN using TBHP (*tert*-butylhydroperoxide) in decane as oxidant and Ti-ALSBA-15 as a catalyst [54]. Some literature data and reaction conditions with CH, CHO, CHD, CK, and CHA substrates are listed in Table 1.

In the present contribution, we report the preparation and characterization of new molecular and resin-supported Mo- and W-based Keggin-type catalysts and their catalytic performance for the production of AA starting from CH. The main objective of the presented research was to evaluate a greener process, avoiding the use of organic solvent, using a new family of grafted catalysts and minimizing the catalyst loading. Different starting substrates for AA production were tested, in order to gain a better insight into the oxidation mechanism, especially by comparison between molecular and grafted catalysts.

**Table 1.** Reaction conditions for the preparation of adipic acid from CH, CHO, CHD, CHK, CHA (see footer for abbreviations)—Some literature data with Mo, W-based polyoxometalates (POMs) and mesoporous catalysts.

Sub.	Cat.	Cat/Sub Loading	Ox. Agent (eq)	T (°C)	Time (h)	AA Yield (%)	Sub Conv (%)	Ref.
CH	Na <sub>2</sub> WO <sub>4</sub> ·2H <sub>2</sub> O [CH <sub>3</sub> ( <i>n</i> -C <sub>8</sub> H <sub>17</sub> ) <sub>3</sub> N]HSO <sub>4</sub>	1%	A	75–90	8	90	>99	[40]
CH	Na <sub>2</sub> WO <sub>4</sub> + ILs	2.5%	4.4 A	reflux	10	100	89–97	[55]
CHK CHA	H <sub>2</sub> WO <sub>4</sub> + ILs	1%	3.3 A 4.4 A	90	20	90	>99	[35]
CH	H <sub>2</sub> WO <sub>4</sub> + IL	2%	4.4 A	73–87	12	85–96	n.d.	[56]
CH	H <sub>4</sub> SiW <sub>12</sub> O <sub>40</sub>	2%	5 A	US (25 kHz)	4	92		[57]
CHA	(C <sub>4</sub> H <sub>9</sub> N) <sub>3</sub> [PMo <sub>12</sub> O <sub>40</sub> ]	0.02%	3 A	reflux	17	18	>99	[39]
CHA CHK	H <sub>3</sub> PMo <sub>12</sub> O <sub>40</sub> NiPMo <sub>12</sub> O <sub>40</sub> CoPMo <sub>12</sub> O <sub>40</sub>	0.5%	1 A	90	14	17–30 17–32	>99	[36]
CHK CHA	H <sub>3–2x</sub> Ni <sub>x</sub> PMo <sub>12</sub> O <sub>40</sub> (NH <sub>4</sub> ) <sub>3–2x</sub> Ni <sub>x</sub> PMo <sub>12</sub> O <sub>40</sub> (x = 0.0–1.5)	0.1–0.4%	1 A	90	20	34–45	>99	[38]
CHK CHA	H <sub>3–2x</sub> Co <sub>x</sub> PMo <sub>12</sub> O <sub>40</sub>	0.15–0.66%	1 A	90	20	30–50	>99	[37]
CHD CHO CHK CHA	Ti-Y zeolites	sub/cat mass ratio = 9.7	4 A	80	24	13–39 44 78 70	24–60 59 36	[42]
CH	Ti-MMM-2 Ce-SBA-15	5 mmol CH 50 mg cat	3.6 A	80	72	10–30	>99	[51]
CH CHO CHD	TAPO-5	62 mmol 0.5 g cat	3.5 A	80	72 24 24	30 40 42	>99 >99 >72	[52]
CHD CHO	Ti-ALSBA-15 + 10 mL CH <sub>3</sub> CN	7 mmol sub 0.1 g	3 B	80	48	50–88 94	56–98 84	[53]
CH		7.8%	3 A	70	24	80	7	[58]
			1.5 B	80	2	10	15	
CHO CHD	Ti(16)Al(DS)SBA + 10 mL CH <sub>3</sub> CN	9.7%	3 B	80	48	94	84	[54]
CH		9.7–19.4%	4B		24–48	76–96	33–88	
							40–84	

CH = cyclohexene, CHA = cyclohexanol, CHK = cyclohexanone, CHO = cyclohexene oxide, A = aqueous H<sub>2</sub>O<sub>2</sub>, B = TBHP in decane AA: adipic acid, US = ultrasound, IL= ionic liquid.

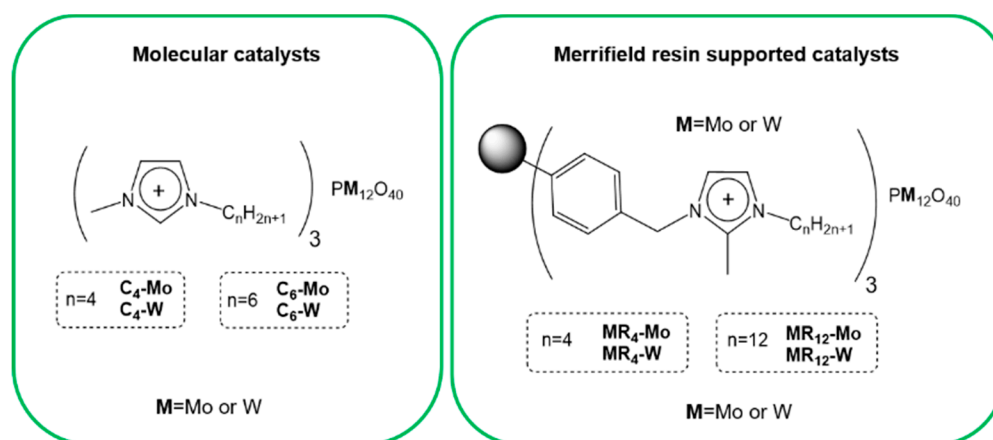
## 2. Results and Discussion

### 2.1. Synthesis and Characterization of the Prepared Catalysts

#### 2.1.1. Synthesis

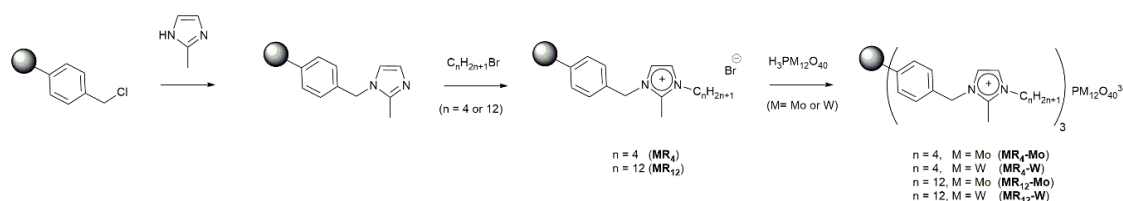
Four molecular catalysts, (Scheme 2, left), were straightforwardly prepared by the reaction of the corresponding ionic liquid (1-hexyl-3-methylimidazolium bromide or 1-butyl-3-methylimidazolium

bromide) and phosphomolybdic or phosphotungstic acid. The four isolated complexes are composed by a  $[\text{PM}_{12}\text{O}_{40}]^{3-}$  ( $\text{M} = \text{Mo}$  or  $\text{W}$ ) surrounded by three alkylmethylimidazolium cations.



Scheme 2. Catalysts used.

The synthesis of the polymer-supported catalysts (Scheme 2, right) was achieved as shown in Scheme 3. Merrifield resins were used as polymeric supports. The resins were modified to obtain two different types of imidazolium-functionalized supports ( $\text{MR}_4$  or  $\text{MR}_{12}$ ) in two steps (see Scheme 3). The first step consisted of the addition of 2-methylimidazole in the presence of a base to the Merrifield resin, leading to the  $\text{MR}_{\text{Im}}$  [59]. The imidazole-functionalized intermediate  $\text{MR}_{\text{Im}}$  was further treated in the second step with the appropriate alkyl bromide to obtain the desired imidazolium moieties ( $\text{MR}_4$  and  $\text{MR}_{12}$ ). The different alkyl chain lengths were expected to increase the lipophilicity of the catalytic object, enhancing the catalyst compatibility with the apolar substrate relatively to the water present in the reaction media since carried by the oxidant ( $\text{H}_2\text{O}_2$  in water). In the last step, the POMs ( $[\text{PMo}_{12}\text{O}_{40}]^{3-}$  or  $[\text{PW}_{12}\text{O}_{40}]^{3-}$ ) were then immobilized by simple ion exchange adding the corresponding heteropolyacids ( $\text{H}_3[\text{PMo}_{12}\text{O}_{40}]$  or  $\text{H}_3[\text{PW}_{12}\text{O}_{40}]$ ). All the synthesized catalysts were characterized by FTIR and elemental analysis.



Scheme 3. Synthetic procedure for the preparation of the heterogeneous catalysts.

### 2.1.2. Characterization

#### • Infrared (IR) Spectroscopy

The IR spectra of the molecular catalysts  $\text{C}_n\text{-M}$  ( $n=4,6$ ;  $\text{M}=\text{Mo}, \text{W}$ ) were assigned according to the literature data [60–63]. The main characteristic features of the Keggin structure were observed at  $1078\text{ cm}^{-1}$  ( $\nu_{\text{as}} \text{P}-\text{O}_a$ ),  $970\text{ cm}^{-1}$  ( $\nu_{\text{as}} \text{M}-\text{O}_d$ ),  $885\text{ cm}^{-1}$  ( $\nu_a \text{M}-\text{O}_d-\text{M}$ ), and  $771\text{--}777\text{ cm}^{-1}$  ( $\nu_{\text{as}} \text{M}-\text{O}_c-\text{M}$ ) for both  $\text{M}$  ( $\text{W}$  and  $\text{Mo}$ ). For the catalysts grafted on Merrifield resins  $\text{MR}_n\text{-M}$  ( $n = 4, 12$ ;  $\text{M}=\text{Mo}, \text{W}$ ), the IR analysis showed the characteristics bands of the 2-methylimidazolium cation,  $1420\text{--}1490\text{ cm}^{-1}$ . The final POM-containing resins exhibit characteristic IR bands at  $1060, 955, 880,$  and  $795\text{--}802\text{ cm}^{-1}$  for  $\text{MR}_4\text{-Mo}$  and  $\text{MR}_{12}\text{-Mo}$ , and at  $1080, 975, 890,$  and  $795\text{--}810\text{ cm}^{-1}$  for  $\text{MR}_4\text{-W}$  and  $\text{MR}_{12}\text{-W}$ , corresponding to the Keggin anions (Figure 1 shows the specific area corresponding to the POM backbone for  $\text{C}_6\text{-Mo}$ ,  $\text{MR}_{12}\text{-Mo}$  and the corresponding starting  $\text{H}_3[\text{PMo}_{12}\text{O}_{40}]$ , proving that the POM structure remains unchanged when grafted).

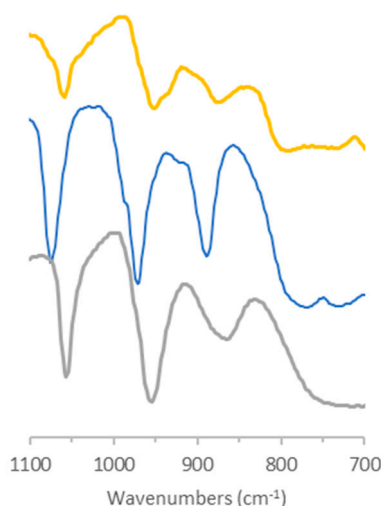


**Figure 1.** Infrared (IR) spectra of the zone of POM vibrations for the commercial  $\text{H}_3\text{PMo}_{12}\text{O}_{40}$  precursor (grey),  $\text{C}_6\text{-Mo}$  molecular catalyst (blue) and  $\text{MR}_{12}\text{-Mo}$  grafted catalyst (orange).

- $^{31}\text{P}$  Nuclear Magnetic Resonance (NMR) Spectroscopy

The  $^{31}\text{P}$  NMR spectra of  $\text{C}_4\text{-Mo}$  and  $\text{C}_6\text{-Mo}$  salts in the solution exhibit a characteristic peak at  $-4.15$  ppm, while those of  $\text{C}_4\text{-W}$  and  $\text{C}_6\text{-W}$  salts show a peak at  $-15.5$  ppm, in accordance with the literature data [64,65]. In the solid-state  $^{31}\text{P}$  NMR spectrum of the Mo-grafted catalysts (Figure 2), the resonance is shifted to  $-3.5$  ppm in case of  $\text{MR}_4\text{-Mo}$ , while two resonances at  $-1.9$  and  $-3.5$  ppm are observed for  $\text{MR}_{12}\text{-Mo}$ . Likewise, in the case of the W catalysts (Figure 3), one resonance is observed for  $\text{MR}_4\text{-W}$  (at  $-15.1$  ppm) and two for  $\text{MR}_{12}\text{-W}$  (at  $-12.4$  and  $-15.2$  ppm). The similar behavior of both POMs seems to depend on the length of the imidazolium substituent and not on the quality of the Keggin POM precursor (the  $^{31}\text{P}$  NMR in  $\text{D}_2\text{O}$  of the commercial Mo and W precursors displayed only one signal at  $-3.9$  and  $-15.3$  ppm, respectively). The observed behavior indicates the presence of different cation-dependent interactions at the resin surface, the two simultaneously observed species possibly corresponding to species located in two different sites (i.e., closer to or farther from the imidazolium moiety) [66,67].

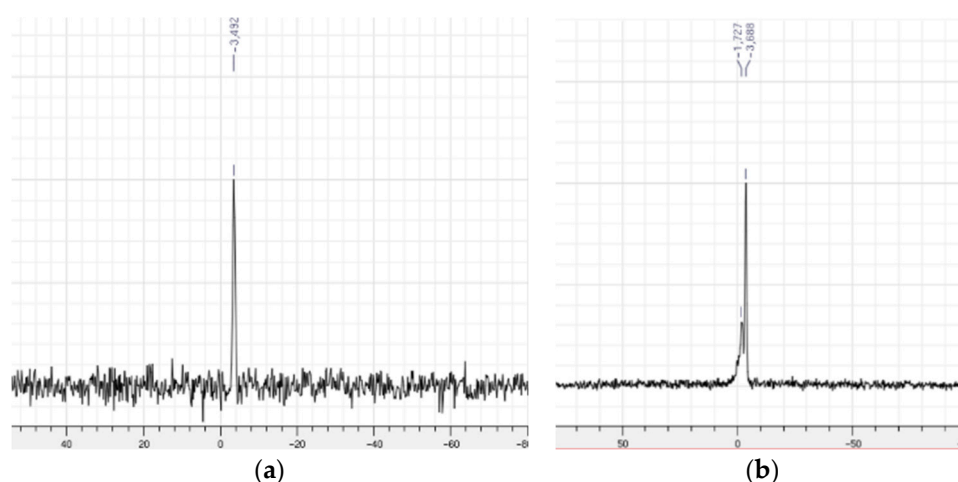


**Figure 2.** Solid-state  $^{31}\text{P}$  NMR of  $\text{MR}_4\text{-Mo}$  (a) and  $\text{MR}_{12}\text{-Mo}$  (b) supported catalysts.

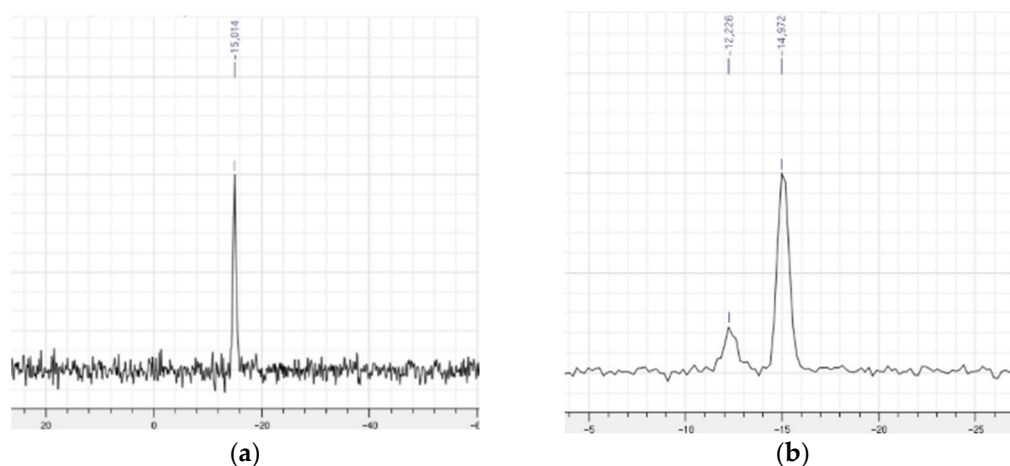


**Figure 3.** Solid-state  $^{31}\text{P}$  NMR of  $\text{MR}_4\text{-W}$  (a) and  $\text{MR}_{12}\text{-W}$  (b) supported catalysts.

- Elemental and Thermogravimetric Analyses

The EA data of the grafted resins show that 32% of Cl from the  $-\text{CH}_2\text{Cl}$  pending functions has been replaced by the 2-methylimidazolium function.

The metal loadings were determined from TG analyses. The residue after thermal treatment was identified as  $\text{P}_2\text{O}_5$  and  $\text{MO}_3$  ( $\text{M} = \text{Mo}$  or  $\text{W}$ ), see Table 2. Figure 4 shows an illustrative example of the TG curve for  $\text{MR}_4\text{-W}$ .

**Table 2.** CHN elemental analyses and metal loading.

EA Data	C (%)	H (%)	N (%)	Cl (%)	M (Mo or W) Loading ( $\mu\text{mol}$ POM/g of Polymer) *
MR	79.1	6.4	-	14.5	-
$\text{MR}_{\text{im}}$	74.6	8.4	6.9	10.1	-
$\text{MR}_4\text{-Mo}$	59.5	6.8	5.0	n.d.	66.7
$\text{MR}_4\text{-W}$	55.9	6.0	4.5	n.d.	12.3
$\text{MR}_{12}\text{-Mo}$	40.9	4.1	4.3	n.d.	55.6
$\text{MR}_{12}\text{-W}$	30.0	3.0	3.5	n.d.	18.9

n.d. = not determined, \* based on the TG analyses.

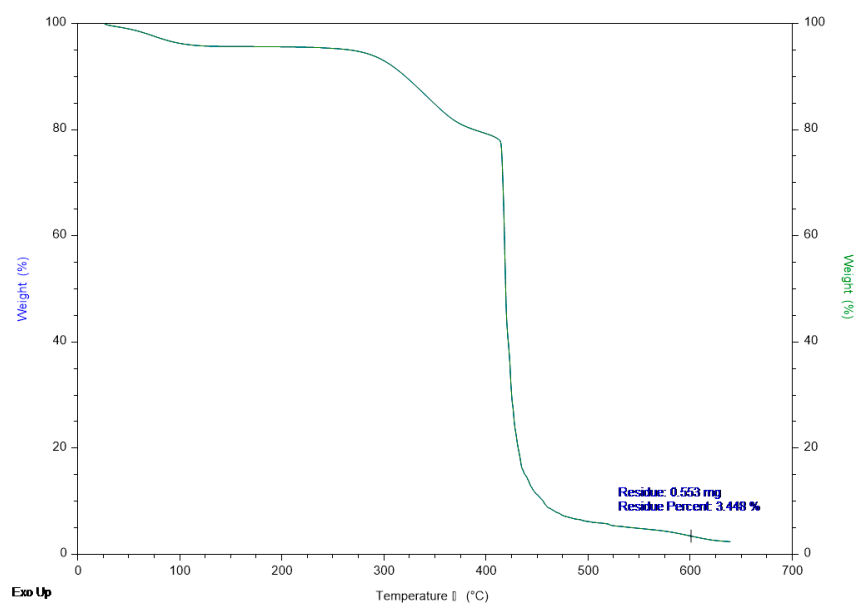
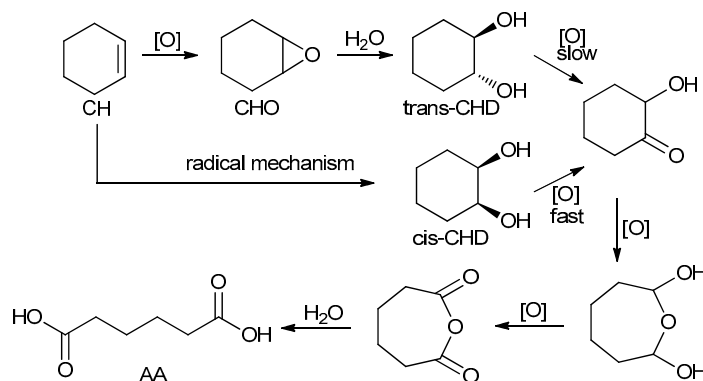


**Figure 4.** Thermogravimetric curve of  $\text{MR}_4\text{-W}$ .

## 2.2. Catalysis

The transformation of CH to AA is reported to involve olefin epoxidation, alcohol oxidations, and Baeyer-Villiger oxidation (Scheme 4) [52].



**Scheme 4.** Steps for the oxidation of CH to AA in the presence of TAPO-5 catalyst. Adapted from [52].

For this reason, we studied the AA formation from different starting compounds (CH, CHO, CHD), using molecular and grafted catalysts. CHO and CHD were used as substrates since they are intermediates in the formation of AA from CH. The formation of the CHD intermediate has also been monitored when starting from CH or CHO (see results in Table 3).

**Table 3.** Data of oxidation reactions for AA production starting from different substrates (CH, CHO, CHD) and different catalysts.

	Molecular Catalysts				Grafted Catalysts			
	C <sub>4</sub>		C <sub>6</sub>		MR <sub>4</sub>		MR <sub>12</sub>	
	Mo	W	Mo	W	Mo	W	Mo	W
%Cat <sup>a</sup>	0.025				0.004	0.007	0.003	0.001
CH as substrate								
CH conv. <sup>b</sup>	65	75	61	68	58	61	56	73
AA yield <sup>c</sup>	46	61	42	50	33	43	30	51
CHD form <sup>d</sup>	15	12	11	17	24	17	19	20
CHO as substrate								
CHO conv. <sup>e</sup>	>99				>99			
AA yield <sup>c</sup>	36	47	32	43	28	33	21	36
CHD form <sup>d</sup>	25	26	29	24	28	23	32	35
CHD as substrate								
CHD conv. <sup>f</sup>	>99				71	94	79	95
AA yield <sup>c</sup>	74	72	58	63	46	60	41	56

<sup>a</sup> Molar ratio (in percentage) relative to the substrate. <sup>b</sup> CH conversion (in %) after t = 3 days, T = 333 K, 4 eq of H<sub>2</sub>O<sub>2</sub> were added in small portions. <sup>c</sup> isolated AA yield (in %). <sup>d</sup> CHD formation (%) based on GC. <sup>e</sup> CHO conversion (in %) after t = 1 day, T = 333 K, 2 eq of H<sub>2</sub>O<sub>2</sub> were added at the beginning of the reaction. <sup>f</sup> CHD conversion (in %) after t = 3 days, T = 333 K, 2 eq of H<sub>2</sub>O<sub>2</sub> were added at the beginning of the reaction.

### • Swelling Tests

In order to verify whether all the MR-supported POMs are accessible to the substrates under organic solvent-free conditions, swelling tests were performed on non-treated MR. Heating the MR in the presence of CH or CHO led to a mass increase by ca. 2% in the case of CH and 8% in the case of CHO, indicating substrate incorporation into the polymer pores and, therefore, catalyst accessibility without organic solvent. This feature is of great importance since it justifies the use of MR as a support in the catalytically solvent-free processes.

- Classical Conditions

Initial tests were performed with the molecular catalysts  $C_n\text{-M}$  ( $n = 4$  or  $6$ ,  $M = \text{Mo}$  or  $\text{W}$ ;  $0.025$  mol% vs. substrate), i.e., a 40 times lower catalyst loading than that reported for  $\text{Na}_2\text{WO}_4$  [40]. All the catalysts were insoluble in the reaction media, but became partially soluble as the reactions evolved, better solubilization was observed for the W-based ones.

- CH as the Substrate

After 60 min, the CH conversion was between 7 and 10% (analyzed by GC) with a low selectivity towards CHO (3%). After 6.5 h, all the molecular catalysts provided a 5–8% selectivity towards CHO with a CH conversion between 12 and 18%. No CHD was observed in the organic layer. The slow conversion is certainly due to the low catalyst loading and to the mild reaction conditions compared to those described in the reference study [35]. After 24 h, however, reasonable conversions were achieved and CHO was no longer detected by GC whereas CHD was present (see Table 1). AA was isolated as a solid in relatively good yields. As stated in several mechanistic studies [52], the species unidentified by GC might correspond to the product of Baeyer Villiger oxidation (see Scheme 4). The observation that CHO is formed and then consumed indicates that this is involved in the AA formation mechanism, via the conversion to CHD.

The homogeneous  $C_n\text{-W}$  catalysts were more active than the corresponding  $C_n\text{-Mo}$ , with AA isolated yields ca. 10% higher on average (see Table 1). Control experiments without catalyst or in the presence of the commercial MR yielded only a very low amount of cis and trans-CHD (<7%) after 24 h. The shorter carbon chain on the imidazolium cation afforded better results. The same trend was previously observed for the same reaction with  $(\text{Hgly})_3[\text{PM}_{12}\text{O}_{40}]$  ( $M = \text{Mo}$ ,  $\text{W}$ ; gly = glycine) [68] or for the cyclooctene epoxidation with alkylpyridinium salts of  $[\text{PMo}_{12}\text{O}_{40}]^{3-}$  [61]. The stirred biphasic reaction medium appeared as an emulsion, possibly stabilized by the solid POM salt (Pickering-type) [69–72].

For the grafted version of the catalysts, the W-based were again more active, despite the lower W content in the case of  $\text{MR}_{12}\text{-W}$  than for  $\text{MR}_{12}\text{-Mo}$  (see Table 1). In contrast to the molecular catalysts, the longer chain on the imidazolium cation led to greater activity. This could be linked to a better “solubilization” of the substrate near the catalyst active site.

- CHO as the Substrate

Complete substrate conversion was observed in this case, with the molecular or the grafted catalysts, producing AA after one day in 21–47% isolated yields together with a relatively high amount of *trans*-CHD (Table 1). This experiment shows that the limiting factor is not the formation of CHD, as seen in other studies [52]. The molecular catalysts (especially those based on W) were more selective towards AA than the grafted ones. It seems that the transformation of CHD to AA is quicker in the presence of the molecular catalysts, since less CHD intermediate accumulates.

- CHD as the Substrate

When *trans*-CHD was used as the starting substrate, the reaction produced AA in higher isolated yields (59–74%) than when starting from CH within the same time period. 2-Hydroxycyclohexanone, a known intermediate within the postulated oxidation pathway (Scheme 4), [52] was also observed by GC but not quantified. The  $C_n\text{-M}$  molecular catalysts are highly active (>99% conversion), more than the grafted ones for which the measured conversion is between 71 and 95%. In all the reactions, the W-based catalysts show slightly better performances in terms of activity and AA yields.

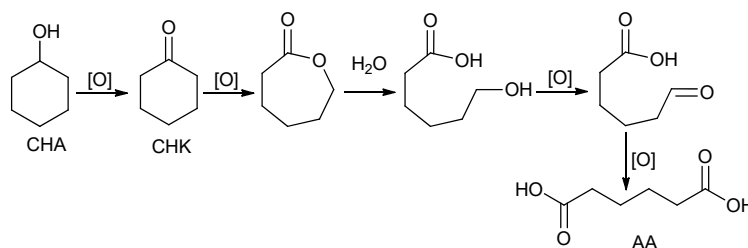
- Recycling

Catalyst recovery and recyclability were investigated for the most active grafted catalyst,  $\text{MR}_{12}\text{-W}$ , and CH as the starting substrate. The IR spectrum of the isolated  $\text{MR}_{12}\text{-W}$  after the first experiment exhibited no change, except for the presence of additional vibrations attributed to CHD. After the 2nd

run, the CH conversion was 54% and the AA yield was 29%. The lower activity after reuse could result from the grafted catalyst inhibition by the presence of CHD within the resin.

- CHK/CHA as the Substrate

In order to mimic a greener industrial process (replacing the traditionally used and environmentally harmful oxidants) the most active molecular catalyst  $C_4\text{-W}$  (0.025% loading) was also tested for the oxidation of CHK and CHA by  $H_2O_2$  (Scheme 5), leading after 24 h to isolated AA yields of 41% and 35% respectively. These results show that  $C_4\text{-W}$  is less active than  $H_2WO_4$  and certain Dawson POMs (58 and 59% with 0.5–2% cat loading with CHA as the substrate) [73], quite similar to  $(NH_4)_x A_y PMO_{12}O_{40}$  ( $A^{n+} = Sb^{3+}, Bi^{3+}, Sn^{2+}$ ) species with CHK as the substrate and better with CHA with a lower POM/substrate ratio [74] but more active than other described POMs (see Table 1), and, therefore, also seems promising for the solvent-free oxidation of CHK and CHA [35].



**Scheme 5.** Oxidation steps of CHA and CHK to AA in the presence of  $H_2WO_4$  catalyst. Adapted from [2].

### 3. Materials and Methods

#### 3.1. Materials

1-Hexyl-3-methylimidazolium bromide (Aldrich, Saint Louis, MO, USA),  $H_3PMO_{12}O_{40} \cdot 26H_2O$  (99.9% Merck, Kennallsburg, NJ, USA),  $H_3PW_{12}O_{40} \cdot 15H_2O$  (purum, Aldrich), 1-methylimidazole (Aldrich), bromobutane (Aldrich), bromododecane (Aldrich), Merrifield resin (Aldrich), EtOH (Aldrich), DMF (Aldrich), dichloromethane (Aldrich), Acetone (Aldrich), Cyclohexene (Aldrich), 35%  $H_2O_2$  (Acros, Geel, Belgium) were used as received

#### 3.2. Physical Methods

Elemental analyses (EA) were provided by the Analytical Services Laboratory of LCC, Toulouse. The thermogravimetric analyses (TGA) were performed on a SETARAM TGA 92-16.18 thermal analyzer. The sample was placed into an alumina crucible and heated at  $0.83 \text{ K} \cdot \text{s}^{-1}$  in a reconstituted air flow from  $25 \text{ }^\circ\text{C}$  to  $600 \text{ }^\circ\text{C}$ . An empty crucible was used as a reference. The POM percentage in the grafted species was calculated from the percentage of residue measured in the TGA traces divided by the molar mass of  $PM_{12}O_{38.5}$ .

Infrared spectra were recorded using the ATR technique with a Perkin Elmer FTIR/FIR 400 spectrometer.

A Bruker Avance DPX-300 spectrometer was used to record  $^{31}\text{P}$  NMR spectra in the solution at 121.5 MHz. All solid-state  $^{31}\text{P}$  NMR experiments were recorded on a Bruker Avance 400 spectrometer equipped with a 3.2 mm probe. Samples were spun at 16 kHz at the magic angle using  $ZrO_2$  rotors. For  $^{31}\text{P}$  MAS single pulse experiments, small flip angle ( $\sim 30^\circ$ ) were used with recycling delays of 20 s.  $^{31}\text{P}$ -CP/MAS spectra were recorded with a recycle delay of 3 s and contact times of 2 ms.  $^{31}\text{P}$  chemical shifts were referenced to an external 85%  $H_3PO_4$  sample.

All the catalytic reactions were followed by gas chromatography on an Agilent 6890 A chromatograph equipped with FID detector, a HP5-MS capillary column ( $30 \text{ m} \times 0.25 \text{ mm} \times 0.25 \text{ }\mu\text{m}$ ) and automatic sampling, or on a Fisons GC 8000 chromatograph equipped with FID detector and with a SPB-5 capillary column ( $30 \text{ m} \times 0.32 \text{ mm} \times 0.25 \text{ }\mu\text{m}$ ).

The GC parameters were quantified with authentic samples of the reactants and products. The CH conversion, the CHD formation, and the CHO conversion/formation were calculated from calibration curves ( $r^2 = 0.999$ ) relative to an internal standard (acetophenone). Acetophenone and CHD are present both in the organic and in the water phase at the end of the catalytic experiments. Therefore, extraction with AcOEt was carried out before the GC analysis. The AA yield was calculated from the isolated mass recovered from the filtered reaction mixture at the end of the reaction.

### 3.3. Preparative Part

#### • Molecular Catalysts

1-Hexyl-3-methylimidazolium bromide (1.65 mmol, 0.41 g) was mixed with aqueous  $\text{H}_3\text{PMo}_{12}\text{O}_{40}$  (M = Mo or W) (0.54 mmol, 1.0 g  $\text{H}_3\text{PMo}_{12}\text{O}_{40}$  or 1.55 g  $\text{H}_3\text{PW}_{12}\text{O}_{40}$ ) and stirred for 2 h. Yellow ( $\text{C}_6\text{-Mo}$ ) or white ( $\text{C}_6\text{-W}$ ) solids precipitated immediately. The solid was filtered, washed with acetone and ether and dried in air.

The preparation of the  $\text{C}_4\text{-M}$  (M = Mo or W) catalysts involved the synthesis of the corresponding ionic liquid [75]. 1-methylimidazole (0.05 mol, 4.1 g) and bromobutane (0.05 mol, 6.85 g) were stirred at 70 °C for 24 h in EtOH (20 mL). After the reaction, EtOH was removed by evaporation under reduced pressure. The formation of the corresponding ionic liquid BMImBr was confirmed by IR [76]. BMImBr (4.4 g, 0.02 mol) was directly mixed with aqueous  $\text{H}_3\text{PMo}_{12}\text{O}_{40}$  (M = Mo or W) ( $6.67 \times 10^{-3}$  mol) and stirred for 2 h. A yellow ( $\text{C}_4\text{-Mo}$ ) or white solid ( $\text{C}_4\text{-W}$ ) precipitated immediately. The solid was filtered, washed with acetone and ether and dried in air.

**$\text{C}_4\text{-Mo}$ :** Yield: 10.3 g (69%). EA: calculated for  $\text{C}_{24}\text{H}_{45}\text{Mo}_{12}\text{N}_6\text{O}_{40}\text{P}$  (%), C: 12.9, H: 2.0, N: 3.6, found (%), C: 12.9, H: 1.9, N: 3.7. IR-ATR ( $\text{cm}^{-1}$ ): 1060, 945, 867, 763, 732.  $^{31}\text{P}$  NMR (ppm):  $-4.15$ .

**$\text{C}_4\text{-W}$ :** Yield: 18.6 g (85%). EA: calculated for  $\text{C}_{24}\text{H}_{45}\text{W}_{12}\text{N}_6\text{O}_{40}\text{P}$  (%), C: 8.7, H: 1.4, N: 2.6, found (%), C: 8.9, H: 1.5, N: 2.7. IR-ATR ( $\text{cm}^{-1}$ ): 1053, 945, 870, 775, 722.  $^{31}\text{P}$  NMR (ppm):  $-15.5$ .

**$\text{C}_6\text{-Mo}$ :** Yield: 11.4 g (74%). EA: calculated for  $\text{C}_{30}\text{H}_{57}\text{Mo}_{12}\text{N}_6\text{O}_{40}\text{P}$  (%), C: 15.5, H: 2.4, N: 3.6, found (%), C: 16.0, H: 2.3, N: 3.8. IR-ATR ( $\text{cm}^{-1}$ ): 1078, 970, 885, 771, 732.  $^{31}\text{P}$  NMR (ppm):  $-4.15$ .

**$\text{C}_6\text{-W}$ :** Yield: 17.6 g (78%). EA: calculated for  $\text{C}_{30}\text{H}_{57}\text{Mo}_{12}\text{N}_6\text{O}_{40}\text{P}$  (%), C: 10.7, H: 1.7, N: 2.5, found (%), C: 10.8, H: 1.6, N: 2.5. IR-ATR ( $\text{cm}^{-1}$ ): 1072, 969, 885, 777, 726.  $^{31}\text{P}$  NMR (ppm):  $-15.5$ .

#### • Grafted Catalysts

The Merrifield resin (1.4–1.6 mmol Cl/g, 5.6–6.4 mmol, 4 g), 2-methylimidazole (0.05 mol, 4 g), and  $\text{Na}_2\text{CO}_3$  (0.01 mol, 1.3 g) were stirred in DMF (20 mL) at 80 °C during 24 h [77]. After washing the resin with dichloromethane (to remove the organic compounds) and then in water until neutral pH, the resin was dried in air. This resin was then placed with 5 mL bromobutane (**MR<sub>4</sub>-**) or bromododecane (**MR<sub>12</sub>-**) and stirred for 72 h at 80 °C. The resin was then washed with dichloromethane, ethanol, and acetone. Finally, it was treated with 5 mL of aqueous solution of  $\text{H}_3\text{PMo}_{12}\text{O}_{40}$  ( $5 \times 10^{-5}$  mol, 0.09 g) or  $\text{H}_3\text{PW}_{12}\text{O}_{40}$  ( $5 \times 10^{-5}$  mol, 0.15 g). After filtration and washing with distilled water and acetone, around 4 g of light yellow resins (**MR<sub>4</sub>-Mo**, **MR<sub>4</sub>-W**, **MR<sub>12</sub>-Mo**, **MR<sub>12</sub>-W**) were obtained.

**MR<sub>4</sub>-Mo:** EA: found (%), C: 59.5, H: 6.8, N: 5.0. TGA (residue) 11.9%. Mo loading ( $\mu\text{mol POM/g}$  of polymer): 66.7. IR-ATR ( $\text{cm}^{-1}$ ): 1060, 953, 878, and 802.  $^{31}\text{P}$  NMR (ppm):  $-3.5$ .

**MR<sub>4</sub>-W** EA: found (%), C: 55.9, H: 6.0, N: 4.5. TGA (residue) 3.5%. W loading ( $\mu\text{mol POM/g}$  of polymer): 12.3. IR-ATR ( $\text{cm}^{-1}$ ): 1079, 975, 894, and 811.  $^{31}\text{P}$  NMR (ppm):  $-15.1$ .

**MR<sub>12</sub>-Mo** EA: found (%), C: 40.9, H: 4.1, N: 4.3. TGA (residue) 9.99%. Mo loading ( $\mu\text{mol POM/g}$  of polymer): 55.6. IR-ATR ( $\text{cm}^{-1}$ ): 1060, 952, 876, and 794.  $^{31}\text{P}$  NMR (ppm):  $-1.9$ ,  $-3.5$ .

**MR<sub>12</sub>-W** EA: found (%), C: 30.0, H: 3.0, N: 3.5. TGA (residue) 5.3%. W loading ( $\mu\text{mol POM/g}$  of polymer): 18.9. IR-ATR ( $\text{cm}^{-1}$ ): 1078, 974, 893, and 797.  $^{31}\text{P}$  NMR (ppm):  $-12.4$ ,  $-15.2$ .

### 3.4. Swelling Test for MR

The MR (0.5 g) was placed in a glass test tube with stopper and CH or CHO was added. The reaction mixture was heated at 60 °C for 6 h. The mixture was filtered and the recovered resin was dried in air and weighted.

### 3.5. General Procedure for Catalytic Oxidation to AA

#### 3.5.1. CH Oxidation (Procedure A)

A round-bottom flask equipped with a magnetic stirring bar and a reflux condenser was charged with CH (80 mmol, 8 mL), acetophenone (3.5 mmol, 0.4 mL), and catalyst (0.02 mmol of molecular catalyst or 0.06 g of grafted catalyst). After the stirred reaction mixture reached 60 °C, H<sub>2</sub>O<sub>2</sub> (320 mmol, 31.1 g, 35%) was added and stirring was continued for 72 h. The final mixture was filtered and the filtrate was left to stand in the refrigerator for one day. The resulting white precipitate was filtered and identified as AA by IR, NMR, and DSC.

#### 3.5.2. CHO Oxidation (Procedure B)

Similar to *procedure A*, with a reaction time of 24 h and 2 eq of H<sub>2</sub>O<sub>2</sub> (160 mmol, 35%).

#### 3.5.3. CHD Oxidation (Procedure C)

Similar to *procedure A*, with a reaction time of 72 h and 2 eq of H<sub>2</sub>O<sub>2</sub> (160 mmol, 35%).

#### 3.5.4. Recycling of the Resins

The resins were isolated at the end of the catalytic reaction, washed with diethylether at room temperature, and dried under ambient air.

#### 3.5.5. CHK or CHA Oxidation (Procedure D)

A round-bottom flask equipped with a magnetic stirring bar and a reflux condenser was charged with cyclohexanone (80 mmol, 7.85 g) or cyclohexanol (80 mmol, 8.0 g) and 10 mL of water. Acetophenone (3.5 mmol, 0.4 mL) was added as an internal standard and the catalyst (0.02 mmol) was added. After the stirred reaction mixture reached 80 °C, H<sub>2</sub>O<sub>2</sub> (320 mmol, 31.1 g, 35%) was added and stirring was continued for 24 h. The homogeneous solution was allowed to stand at 0 °C for 12 h, and the resulting precipitate was separated by filtration and washed with 20 mL of cold water. The product was dried in a vacuum to give AA as a solid.

## 4. Conclusions

Immobilization of the Keggin phosphomolybdate and phosphotungstate on functionalized Merrifield resins has led to the development of new heterogeneous catalysts for AA production in a one-step procedure from CH. Different intermediates were detected and the key steps could be determined by running comparative oxidation tests from each one of the possible intermediates. The substrate itself is able to swell the MR allowing access to all catalytic sites without the use of the classical swelling organic solvents. This atom economical methodology obeys a few of the green chemistry principles (*greener oxidant*, *no phase transfer catalysts*, *no organic solvents added* (safer reagents and atom economy), *minimal catalyst loading* and recyclability). The developed protocol is straightforward, safe, and environmentally benign and can be extended to a variety of other POM-based catalyzed oxidations.

**Author Contributions:** Conceptualization, J.P. and D.A.; methodology, J.P. and D.A.; validation, J.P., D.A. and R.P.; formal analysis and investigation, J.P., D.A.; writing—Original draft preparation, J.P., D.A.; writing—Review and editing, J.P., D.A. and R.P.

**Funding:** The research leading to these results has received funding from the European Union Seventh Framework Programme (FP7 2007–2013) as the project “Diligent search for chemical bio-sources: Solvent-free homogeneous and heterogeneous oxidation processes catalyzed by polyoxometalates”, under grant agreement n°291823 Marie Curie FP7-PEOPLE-2011-COFUND (The new International Fellowship Mobility Programme for Experienced Researchers in Croatia-NEWFELPRO).

**Acknowledgments:** The authors acknowledge LCC-CNRS for elemental analyses and especially. Y. Coppel for the NMR and the Department of Chemistry of IUT at Castres for the facilities in synthesis, catalysis, and TGA.

**Conflicts of Interest:** The authors declare no conflict of interest.

## References

1. Viers, V.; Brendt, D. *Polymer Data Handbook*; Oxford University Press: Oxford, UK, 1999; p. 189.
2. Van de Vyver, S.; Roman-Leshkov, Y. Emerging catalytic processes for the production of adipic acid. *Catal. Sci. Technol.* **2013**, *3*, 1465–1479. [[CrossRef](#)]
3. Cavani, F.; Alini, S. *Synthesis of Adipic Acid: On the Way to More Sustainable Production in Sustainable Industrial Processes*; Cavani, F., Centi, G., Perathoner, S., Trifiró, F., Eds.; WILEY-VCH Verlag GmbH & Co. KGaA: Weinheim, Germany, 2009; pp. 367–425. ISBN 978-3-527-31552-9.
4. Buchner, W.; Schliebs, R.; Winter, G.; Buchel, K.H. *Industrielle Anorganische Chemie*, 2nd ed.; VCH Weinheim: Weinheim, Germany, 1986.
5. Kroeze, C.; Mosier, A. New estimates for Emissions of Nitrous Oxide. In *Non-CO<sub>2</sub> Greenhouse Gases: Scientific Understanding, Control and Implementation*; van Ham, J.M., Baede, A.P., Meyer, L.A., Ybema, R., Eds.; Kluwer Academic Publishers: Dordrecht, The Netherlands, 1999; pp. 45–64. ISBN 978-0-7923-6199-2.
6. Hermans, I.; Spier, S.E.; Neuenschwander, U.; Turra, N.; Baiker, A. Selective oxidation catalysis: Opportunities and challenges. *Top. Catal.* **2009**, *52*, 1162–1174. [[CrossRef](#)]
7. Shimizu, A.; Tanaka, K.; Fujimori, M. Abatement technologies for N<sub>2</sub>O emissions in the adipic acid industry. *Chemosphere Glob. Chang. Sci.* **2000**, *2*, 425–434. [[CrossRef](#)]
8. Reimer, R.A.; Slaten, C.S.; Seapan, M.; Lower, M.W.; Tomlinson, P.E. Abatement of N<sub>2</sub>O emissions produced in the adipic acid industry. *Environ. Prog.* **1994**, *13*, 134–137. [[CrossRef](#)]
9. Bart, J.C.J.; Cavallaro, S. Transitioning from Adipic Acid to Bioadipic Acid. 1, Petroleum-Based Processes. *Ind. Eng. Chem. Res.* **2015**, *54*, 1–46. [[CrossRef](#)]
10. Cavani, F. Catalytic selective oxidation faces the sustainability challenge: Turning points, objectives reached, old approaches revisited and solutions still requiring further investigation. *J. Chem. Technol. Biotechnol.* **2010**, *85*, 1175–1183. [[CrossRef](#)]
11. Brégeault, J.-M. Transition-metal complexes for liquid-phase catalytic oxidation: Some aspects of industrial reactions and of emerging technologies. *Dalton Trans.* **2003**, 3289–3302. [[CrossRef](#)]
12. Jones, C.W. *Applications of Hydrogen Peroxide and Derivatives*; Royal Society of Chemistry: Cambridge, UK, 1999; ISBN 978-0-85404-536-5.
13. Strukul, G. (Ed.) *Catalytic Oxidations with Hydrogen Peroxide as Oxidant*; Kluwer Academic: Dordrecht, The Netherlands, 1992; ISBN 978-0-7923-1771-5.
14. Sheldon, R.A.; Kochi, J.K. *Metal Catalyzed Oxidations of Organic Compounds*; Academic Press: New York, NY, USA, 1981; ISBN 978-0-12-639380-4.
15. Damm, M.; Gutmann, B.; Kappe, C.O. Continuous-Flow Synthesis of Adipic Acid from Cyclohexene Using Hydrogen Peroxide in High-Temperature Explosive Regimes. *ChemSusChem* **2013**, *6*, 978–982. [[CrossRef](#)]
16. Shang, M.; Noel, T.; Su, Y.; Hessel, V. High Pressure Direct Synthesis of Adipic Acid from Cyclohexene and Hydrogen Peroxide via Capillary Microreactors. *Ind. Eng. Chem. Res.* **2016**, *55*, 2669–2676. [[CrossRef](#)]
17. Vural-Gursel, I.; Wang, Q.; Noel, T.; Hessel, V.; Tinge, J.T. Improving Energy Efficiency of Process of Direct Adipic Acid Synthesis in Flow Using Pinch Analysis. *Ind. Eng. Chem. Res.* **2013**, *52*, 7827–7835. [[CrossRef](#)]
18. Shang, M.; Noël, T.; Wang, Q.; Su, Y.; Miyabayashi, K.; Hessel, V.; Hasebe, S. 2- and 3-Stage temperature ramping for the direct synthesis of adipic acid in micro-flow packed-bed reactors. *Chem. Eng. J.* **2015**, *260*, 454–462. [[CrossRef](#)]
19. Wen, Y.; Wang, X.; Wei, H.; Li, B.; Jin, P.; Li, L. A large-scale continuous-flow process for the production of adipic acid via catalytic oxidation of cyclohexene with H<sub>2</sub>O<sub>2</sub>. *Green Chem.* **2012**, *14*, 2868–2875. [[CrossRef](#)]
20. Buonomenna, M.G.; Golemme, G.; De Santo, M.P.; Drioli, E. Direct Oxidation of Cyclohexene with Inert Polymeric Membrane Reactor. *Org. Process Res. Dev.* **2010**, *14*, 252–258. [[CrossRef](#)]

21. Freitag, J.; Nüchter, M.; Ondruschka, B. Oxidation of styrene and cyclohexene under microwave conditions. *Green Chem.* **2003**, *5*, 291–295. [[CrossRef](#)]
22. Misono, M. Unique acid catalysis of heteropoly compounds(heteropolyoxometalates) in the solid state. *Chem. Commun.* **2001**, 1141–1152. [[CrossRef](#)]
23. Kholdeeva, O.A.; Maksimchuk, N.V.; Maksimo, G.M. Polyoxometalate-based heterogeneous catalysts for liquid phase selective oxidations: Comparison of different strategies. *Catal. Today* **2010**, *157*, 107–113. [[CrossRef](#)]
24. Mizuno, N.; Misono, M. Heterogeneous Catalysis. *Chem. Rev.* **1998**, *98*, 199–218. [[CrossRef](#)]
25. Gupta, K.C.; Sutar, A.K.; Lin, C.-C. Polymer-supported Schiff base complexes in oxidation reactions. *Coord. Chem. Rev.* **2009**, *253*, 1926–1946. [[CrossRef](#)]
26. McNamara, C.A.; Dixon, M.J.; Bradley, M. Recoverable Catalysts and Reagents Using Recyclable Polystyrene-Based Supports. *Chem. Rev.* **2002**, *102*, 3275–3300. [[CrossRef](#)]
27. Mizuno, N.; Yamaguchi, K.; Kamata, K. Molecular design of polyoxometalate-based compounds for environmentally-friendly functional group transformations: From molecular catalysts to heterogeneous catalysts. *Catal. Surv. Asia* **2011**, *15*, 68–79. [[CrossRef](#)]
28. Bentaleb, F.; Makrygeni, O.; Brouri, D.; Coelho Diogo, C.; Mehdi, A.; Proust, A.; Launay, F.; Villanneau, R. Efficiency of Polyoxometalate-Based Mesoporous Hybrids as Covalently Anchored Catalysts. *Inorg. Chem.* **2015**, *54*, 7607–7616. [[CrossRef](#)] [[PubMed](#)]
29. Cheng, C.-Y.; Lin, K.-J.; Prasad, M.R.; Fu, S.-J.; Chang, S.-Y.; Shyu, S.-G.; Sheu, H.-S.; Chen, C.-H.; Chuang, C.-H.; Lin, M.-T. Synthesis of a reusable oxotungsten-containing SBA-15 mesoporous catalyst for the organic solvent-free conversion of cyclohexene to adipic acid. *Catal. Commun.* **2007**, *8*, 1060–1064. [[CrossRef](#)]
30. Xiao, Y.; Chen, D.; Ma, N.; Hou, Z.Y.; Hu, M.B.; Wang, C.H.; Wang, W. Covalent immobilization of a polyoxometalate in a porous polymer matrix: A heterogeneous catalyst towards sustainability. *RSC Adv.* **2013**, *3*, 21544–21551. [[CrossRef](#)]
31. Merrifield, R.B. Solid Phase Peptide Synthesis. I. The Synthesis of a Tetrapeptide. *J. Am. Chem. Soc.* **1963**, *85*, 2149–2154. [[CrossRef](#)]
32. Maurya, M.R. Catalytic Applications of Polymer-Supported Molybdenum Complexes in Organic Transformations. *Curr. Org. Chem.* **2012**, *16*, 73–88. [[CrossRef](#)]
33. Da Silva, J.A.L.; Fraústo da Silva, J.J.R.; Pombeiro, A.J.L. Oxovanadium complexes in catalytic oxidations. *Coord. Chem. Rev.* **2011**, *255*, 2232–2248. [[CrossRef](#)]
34. Alini, S.; Babini, P. The Industrial Oxidation of KA Oil to Adipic Acid. In *Handbook of Advanced Methods and Processes in Oxidation Catalysis*; Imperial College Press: London, UK, 2014; pp. 320–333. [[CrossRef](#)]
35. Usui, Y.; Sato, K. A green method of adipic acid synthesis: Organic solvent- and halide-free oxidation of cycloalkanones with 30% hydrogen peroxide. *Green Chem.* **2003**, *5*, 373–375. [[CrossRef](#)]
36. Mazari, T.; Benadji, S.; Tahar, A.; Dermeche, L.; Rabia, C. Liquid-Phase Synthesis of Adipic Acid Using Keggin-Type Phosphomolybdates Catalysts. *J. Mater. Sci. Eng. B* **2013**, *3*, 146–152. [[CrossRef](#)]
37. Benadji, S.; Mazari, T.; Dermeche, L.; Salhi, N.; Cadot, E.; Rabia, C. Clean Alternative for Adipic Acid Synthesis Via Liquid-Phase Oxidation of Cyclohexanone and Cyclohexanol Over  $H_{3-2x}Co_xPMo_{12}O_{40}$  Catalysts with Hydrogen Peroxide. *Catal. Lett.* **2013**, *143*, 749–755. [[CrossRef](#)]
38. Tahar, A.; Benadji, S.; Mazari, T.; Dermeche, L.; Roch-Marchal, C.; Rabia, C. Preparation, Characterization and Reactivity of Keggin Type Phosphomolybdates,  $H_{3-2x}Ni_xPMo_{12}O_{40}$  and  $(NH_4)_{3-2x}Ni_xPMo_{12}O_{40}$ , for Adipic Acid Synthesis. *Catal. Lett.* **2015**, *145*, 569–575. [[CrossRef](#)]
39. Nomiya, K.; Miwa, M.; Sugaya, Y. Catalysis by heteropolyacid—VII. catalytic oxidation of cyclohexanol by dodecamolybdate. *Polyhedron* **1984**, *3*, 607–610. [[CrossRef](#)]
40. Sato, K.; Aoki, M.; Noyori, R. A “Green” Route to Adipic Acid: Direct Oxidation of Cyclohexenes with 30 Percent Hydrogen Peroxide. *Science* **1998**, *281*, 1646–1647. [[CrossRef](#)] [[PubMed](#)]
41. Cavani, F.; Teles, J.H. Sustainability in catalytic oxidation: An alternative approach or a structural evolution? *ChemSusChem* **2009**, *2*, 508–534. [[CrossRef](#)] [[PubMed](#)]
42. Schindler, G.P.; Bartl, P.; Hoelderich, W.F. Oxidative cleavage of cyclohexane derivatives over titanium-containing Y zeolites. *Appl. Catal. A* **1998**, *166*, 267–279. [[CrossRef](#)]
43. Wang, W.; Liu, H.; Ding, G.; Zhang, P.; Wu, T.; Jiang, T.; Han, B. Ru–Cd/Bentonite for the Partial Hydrogenation of Benzene: A Catalyst without Additives. *ChemCatChem* **2012**, *4*, 1836–1843. [[CrossRef](#)]

44. Schwab, F.; Lucas, M.; Claus, P. Ruthenium-catalyzed selective hydrogenation of benzene to cyclohexene in the presence of an ionic liquid. *Angew. Chem. Int. Ed.* **2011**, *50*, 10453–10456. [[CrossRef](#)] [[PubMed](#)]
45. Liu, H.; Jiang, T.; Han, B.; Liang, S.; Wang, W.; Wu, T.; Yang, G. Highly selective benzene hydrogenation to cyclohexene over supported Ru catalyst without additives. *Green Chem.* **2011**, *13*, 1106–1109. [[CrossRef](#)]
46. Jin, M.; Cheng, Z.-M. Oxidative Dehydrogenation of Cyclohexane to Cyclohexene over Mg-V-O Catalysts. *Catal. Lett.* **2009**, *131*, 266–278. [[CrossRef](#)]
47. Patcas, F.; Patcas, F.C. Reaction pathways and kinetics of the gas-phase oxidation of cyclohexane on NiO/ $\gamma$ -Al<sub>2</sub>O<sub>3</sub> catalyst. *Catal. Today* **2006**, *117*, 253–258. [[CrossRef](#)]
48. Zhu, H.; Ge, Q.; Li, W.; Liu, X.; Xu, H. Study of Mn-based Catalysts for Oxidative Dehydrogenation of Cyclohexane to Cyclohexene. *Catal. Lett.* **2005**, *105*, 29–33. [[CrossRef](#)]
49. Soares, J.C.S.; Gonçalves, A.H.A.; Zotin, F.M.Z.; Raddi de Araújo, L.R.; Gaspar, A.B. Cyclohexene to adipic acid synthesis using heterogeneous polyoxometalate catalysts. *Mol. Catal.* **2018**, *458*, 223–229. [[CrossRef](#)]
50. Bohström, Z.; Rico-Lattes, I.; Holmberg, K. Oxidation of cyclohexene into adipic acid in aqueous dispersions of mesoporous oxides with built-in catalytical sites. *Green Chem.* **2010**, *12*, 1861–1869. [[CrossRef](#)]
51. Timofeeva, M.N.; Kholdeeva, O.A.; Jhung, S.H.; Chang, J.-S. Titanium and cerium-containing mesoporous silicate materials as catalysts for oxidative cleavage of cyclohexene with H<sub>2</sub>O<sub>2</sub>: A comparative study of catalytic activity and stability. *Appl. Catal. A* **2008**, *345*, 195–200. [[CrossRef](#)]
52. Lee, S.O.; Raja, R.; Harris, K.D.M.; Tomas, J.M.; Johnson, B.F.J.; Sankar, G. Mechanistic Insights into the Conversion of Cyclohexene to Adipic Acid by H<sub>2</sub>O<sub>2</sub> in the Presence of a TAPO-5 Catalyst. *Angew. Chem. Int. Ed.* **2003**, *42*, 1520–1523. [[CrossRef](#)] [[PubMed](#)]
53. Lapisardi, G.; Chiker, F.; Launay, F.; Nogier, J.P.; Bonardet, J.L. Preparation, characterisation and catalytic activity of new bifunctional Ti-*AlSBA15* materials. Application to a “one-pot” green synthesis of adipic acid from cyclohexene and organic hydroperoxides. *Microporous Mesoporous Mater.* **2005**, *78*, 289–295. [[CrossRef](#)]
54. Lapisardi, G.; Chiker, F.; Launay, F.; Nogier, J.P.; Bonardet, J.L. A “one-pot” synthesis of adipic acid from cyclohexene under mild conditions with new bifunctional Ti-*AlSBA* mesostructured catalysts. *Catal. Commun.* **2004**, *5*, 277–281. [[CrossRef](#)]
55. Gui, J.; Liu, D.; Cong, X.; Zhang, X.; Jiang, H.; Hu, Z.; Sun, Z. Clean synthesis of adipic acid by direct oxidation of cyclohexene with H<sub>2</sub>O<sub>2</sub> catalysed by Na<sub>2</sub>WO<sub>4</sub>·2H<sub>2</sub>O and acidic ionic liquids. *J. Chem. Res.* **2005**, *8*, 520–522. [[CrossRef](#)]
56. Wang, B.; Zhang, Z.; Zhang, X.; Sun, S.; Wu, L.; Xing, R. Efficient and convenient oxidation of cyclohexene to adipic acid with H<sub>2</sub>O<sub>2</sub> catalyzed by H<sub>2</sub>WO<sub>4</sub> in acidic ionic liquids. *Chem. Pap.* **2018**, *72*, 643–649. [[CrossRef](#)]
57. Lin, Z.-P.; Wan, L. Synthesis of Adipic Acid Oxidized by H<sub>2</sub>O<sub>2</sub>-Silicotungstic Acid Under Ultrasonication. *Asian J. Chem.* **2013**, *25*, 6008–6010. [[CrossRef](#)]
58. Chiker, F.; Launay, F.; Nogier, J.P.; Bonardet, J.L. Green epoxidation on Ti-mesoporous catalysts. *Environ. Chem. Lett.* **2003**, *1*, 117–120. [[CrossRef](#)]
59. Santini, R.; Griffith, M.C.; Qi, M. A measure of solvent effects on swelling of resins for solid phase organic synthesis. *Tetrahedron Lett.* **1998**, *39*, 8951–8954. [[CrossRef](#)]
60. Rocchiccioli-Deltcheff, C.; Fournier, M.; Franck, R.; Thouvenot, R. Vibrational investigations of polyoxometalates. 2. Evidence for anion-anion interactions in molybdenum(VI) and tungsten(VI) compounds related to the Keggin structure. *Inorg. Chem.* **1983**, *22*, 207–216. [[CrossRef](#)]
61. Rocchiccioli-Deltcheff, C.; Fournier, M. Catalysis by polyoxometalates. Part 3.—Influence of vanadium(V) on the thermal stability of 12-metallophosphoric acids from in situ infrared studies. *J. Chem. Soc. Faraday Trans.* **1991**, *87*, 3913–3920. [[CrossRef](#)]
62. Aouissi, A.; Abdullah Al-Othman, Z.; Al-Anezi, H. Reactivity of Heteropolymolybdates and Heteropolytungstates in the Cationic Polymerization of Styrene. *Molecules* **2010**, *15*, 3319–3328. [[CrossRef](#)] [[PubMed](#)]
63. Nakashima, T.; Kimizuka, N. Interfacial Synthesis of Hollow TiO<sub>2</sub> Microspheres in Ionic Liquids. *J. Am. Chem. Soc.* **2003**, *125*, 6386–6387. [[CrossRef](#)] [[PubMed](#)]
64. Ganapathy, S.; Fournier, M.; Paul, J.F.; Delevoye, L.; Guelton, M.; Amoureux, J.P. Location of Protons in Anhydrous Keggin Heteropolyacids H<sub>3</sub>PMo<sub>12</sub>O<sub>40</sub> and H<sub>3</sub>PW<sub>12</sub>O<sub>40</sub> by <sup>1</sup>H{<sup>31</sup>P}/<sup>31</sup>P{<sup>1</sup>H} REDOR NMR and DFT Quantum Chemical Calculations. *J. Am. Chem. Soc.* **2002**, *26*, 7821–7828. [[CrossRef](#)]
65. Chen, Y.; Tan, R.; Zheng, W.; Zhang, Y.; Zhao, G.; Yin, D. Dendritic phosphotungstate hybrids efficiently catalyze the selective oxidation of alcohols with H<sub>2</sub>O<sub>2</sub>. *Catal. Sci. Technol.* **2014**, *4*, 4084–4092. [[CrossRef](#)]

66. Chang, T. NMR characterization of the supported 12-heteropoly acids. *J. Chem. Soc. Faraday Trans.* **1995**, *91*, 375–379. [[CrossRef](#)]
67. Edwards, J.C.; Thiel, C.Y.; Benac, B.; Knifton, J.F. Solid-state NMR and FT-IR investigation of 12-tungstophosphoric acid on TiO<sub>2</sub>. *Catal. Lett.* **1998**, *51*, 77–83. [[CrossRef](#)]
68. Ren, S.; Xie, Z.; Cao, L.; Xie, X.; Qin, G.; Wang, J. Clean synthesis of adipic acid catalyzed by complexes derived from heteropoly acid and glycine. *Catal. Commun.* **2009**, *10*, 464–467. [[CrossRef](#)]
69. Guérin, B.; Mesquita Fernandez, D.; Daran, J.-C.; Agustin, D.; Poli, R. Investigation of induction times, activity, selectivity, interface and mass transport in solvent-free epoxidation by H<sub>2</sub>O<sub>2</sub> and TBHP: A study with organic salts of the [PMo<sub>12</sub>O<sub>40</sub>]<sup>3-</sup> anion. *New J. Chem.* **2013**, *37*, 3466–3475. [[CrossRef](#)]
70. Leclercq, L.; Mouret, A.; Proust, A.; Schmitt, V.; Bauduin, P.; Aubry, J.M.; Nardello-Rataj, V. Pickering Emulsion Stabilized by Catalytic Polyoxometalate Nanoparticles: A New Effective Medium for Oxidation Reactions. *Chem.-Eur. J.* **2012**, *18*, 14352–14358. [[CrossRef](#)] [[PubMed](#)]
71. Yang, B.; Leclercq, L.; Schmitt, V.; Pera-Titus, M.; Nardello-Rataj, V. Colloidal tectonics for tandem synergistic Pickering interfacial catalysis: Oxidative cleavage of cyclohexene oxide into adipic acid. *Chem. Sci.* **2019**, *10*, 501–507. [[CrossRef](#)] [[PubMed](#)]
72. Wei, X.-R.; Liu, J.; Yang, Y.; Deng, L. A general approach towards efficient catalysis in Pickering emulsions stabilized by amphiphilic RGO–Silica hybrid materials. *RSC Adv.* **2014**, *4*, 35744–35749. [[CrossRef](#)]
73. Moudjahed, M.; Dermeche, L.; Benadji, S.; Mazari, T.; Rabia, C. Dawson-type polyoxometalates as green catalysts for adipic acid synthesis. *J. Mol. Catal. A Chem.* **2016**, *414*, 72–77. [[CrossRef](#)]
74. Mouheb, L.; Dermeche, L.; Mazari, T.; Benadji, S.; Essayem, N.; Rabia, C. Clean Adipic Acid Synthesis from Liquid-Phase Oxidation of Cyclohexanone and Cyclohexanol Using (NH<sub>4</sub>)<sub>x</sub>A<sub>y</sub>PMo<sub>12</sub>O<sub>40</sub> (A: Sb, Sn, Bi) Mixed Heteropolysalts and Hydrogen Peroxide in Free Solvent. *Catal. Lett.* **2018**, *148*, 612–620. [[CrossRef](#)]
75. Huddleston, J.G.; Visser, A.E.; Reichert, W.M.; Willauer, H.D.; Broker, G.A.; Rogers, R.D. Characterization and comparison of hydrophilic and hydrophobic room temperature ionic liquids incorporating the imidazolium cation. *Green Chem.* **2001**, *3*, 156–164. [[CrossRef](#)]
76. Cha, S.; Ao, M.; Sung, W.; Moon, B.; Ahlström, B.; Johansson, P.; Ouchi, Y.; Kim, D. Structures of ionic liquid–water mixtures investigated by IR and NMR spectroscopy. *Phys. Chem. Chem. Phys.* **2014**, *16*, 9591–9601. [[CrossRef](#)]
77. Poli, E.; Clacens, J.-M.; Pouilloux, Y. Synthesis of peroxophosphotungstate immobilized onto polymeric support as heterogeneous catalyst for the epoxidation of unsaturated fatty esters. *Catal. Today* **2011**, *164*, 429–435. [[CrossRef](#)]

**Sample Availability:** Samples of the compounds are not available from the authors.



© 2019 by the authors. Licensee MDPI, Basel, Switzerland. This article is an open access article distributed under the terms and conditions of the Creative Commons Attribution (CC BY) license (<http://creativecommons.org/licenses/by/4.0/>).